

Theory of tunneling spectroscopy in UPd₂Al₃

David Parker¹ and Peter Thalmeier²

¹Max Planck Institute for the Physics of Complex Systems, Nöthnitzer Str. 38, D-01187 Dresden, Germany

²Max Planck Institute for the Chemical Physics of Solids, Nöthnitzer Str. 40, D-01187 Dresden, Germany

(Dated: November 1, 2018)

There is still significant debate about the symmetry of the order parameter in the heavy-fermion superconductor UPd₂Al₃, with proposals for $\cos(k_3)$, $\cos(2k_3)$, $\sin(k_3)$, and $e^{i\phi}\sin(k_3)$. Here we analyze the tunneling spectroscopy of this compound and demonstrate that the experimental results by Jourdan et al¹ are inconsistent with the last two order parameters, which are expected to show zero-bias conductance peaks. We propose a definitive tunneling experiment to distinguish between the first two order parameters.

PACS numbers:

I. INTRODUCTION

Superconductivity in UPd₂Al₃ with a transition temperature $T_c = 2$ K was discovered in 1991 by Geibel et al², and since that time much experimental and theoretical work has been performed, with a particular aim of establishing the order parameter symmetry. In general, this determination is a crucial first step in understanding the pairing mechanism of a given superconductor, so that large efforts are generally expended in this direction.

Evidence for unconventional or nodal superconductivity in UPd₂Al₃ has emerged from a variety of experiments. Feyerherm et al³ measured the Knight shift in UPd₂Al₃ and found a substantial reduction below T_c , indicative of singlet pairing. In NMR experiments Tou⁴ and Matsuda⁵ found low-temperature nuclear spin lattice relaxation rate T_1^{-1} power law (T^3) behavior, and the absence of a Hebel-Slichter coherence peak below T_c . Both behaviors are characteristic of nodal superconductivity, and in particular the observation of T^3 behavior is strongly suggestive of line nodes in the order parameter. Similar evidence was obtained by Sato⁶, who measured the low-temperature specific heat and found T^2 behavior, also indicative of line nodes. Hiroi et al⁷ measured the low-temperature thermal conductivity and also found T^2 behavior. More recently, Watanabe et al⁸ measured the angle-dependent magnetothermal conductivity and found evidence for a single line node parallel to the basal plane of the hexagonal UPd₂Al₃.

Tunnelling spectroscopy can be a powerful probe of order parameter symmetry. The pioneering work in this field was performed by Blonder, Tinkham and Klapwijk (BTK)⁹, who provided a simple solution to the problem of Andreev reflection¹⁰ in s-wave superconductors in an N-I-S contact, and by Tanaka et al¹¹, who was able to explain the zero-bias conductance peaks (ZBCP) generally observed in tunneling measurements of the high-temperature cuprate superconductors¹². Since that time much theoretical work on tunneling spectroscopy in various materials has been performed; primary references of interest are the book by Tinkham¹³ and the study by Honerkamp and Sigrist¹⁴.

The basic conclusion of Tanaka's original work was that zero-bias conductance peaks are intimately tied in with the phase difference between the pair potentials of the transmitted electron-like and hole-like quasiparticles on the superconducting side of the junction. When this phase difference reaches π , Andreev reflection (resulting in the transmission of two electrons for a single incoming electron) is enhanced and normal reflection diminished, so that the transmission coefficient is increased. This enhancement is most prominent at zero-energy. At increasing tunneling energy barrier height (the thin oxide layer between the superconductor and normal) the normal state conductance decreases, so that the relative conductance, or ratio of su-

perconducting to normal state conductance, increases. It should be noted that while strongly enhanced ZBCPs (diverging in the limit of large barrier height) only result from a π phase difference, significant zero-energy states can be realized in other cases, as in¹⁴. We show below that for the case of interest, substantial amounts of zero-energy states can be realized even for order parameters without the requisite π phase change, when the effects of quasiparticle lifetime are accounted for. The magnitude of these zero-energy states, as well as the height and energy of the quasiparticle coherence peaks, are strong functions of the order parameter, and for the geometry appropriate to UPd₂Al₃, of the normal metal used in the junction, so that a wide range of interesting and informative experimental results can be obtained, offering a definitive resolution to the question of order parameter symmetry in UPd₂Al₃.

II. MODEL

In general, the pair state of a superconductor is described by the Bogoliubov-deGennes equations^{9,11,15,16}:

$$i\hbar \frac{\partial f}{\partial t} = - \left[\frac{\hbar^2 \nabla^2}{2m} + \mu + V(x) \right] f(\mathbf{x}, \mathbf{k}, t) - \Delta(\mathbf{x}, \mathbf{k}) g(x, t) \quad (1)$$

$$i\hbar \frac{\partial g}{\partial t} = \left[\frac{\hbar^2 \nabla^2}{2m} + \mu + V(x) \right] g(\mathbf{x}, \mathbf{k}, t) - \Delta(\mathbf{x}, \mathbf{k}) f(x, t) \quad (2)$$

Here, as in Klapwijk et al¹⁶, we take the f 's as electron wave functions and the g 's as hole wave functions, and note that the solutions to these equations can be written as

$$f(\mathbf{x}, \mathbf{k}, t) = u(\mathbf{k}) \exp(i(\mathbf{k} \cdot \mathbf{r} - Et)/\hbar) \quad (3)$$

$$g(\mathbf{x}, \mathbf{k}, t) = v(\mathbf{k}) \exp(i(\mathbf{k} \cdot \mathbf{r} + Et)/\hbar) \quad (4)$$

where u and v are the well-known BCS coherence factors^{14,16,17}:

$$u(\mathbf{k}) = \sqrt{\frac{1}{2}(1 + \sqrt{E^2 - |\Delta(\mathbf{k})|^2}/E})} \quad (5)$$

$$v(\mathbf{k}) = \sqrt{\frac{1}{2}(1 - \sqrt{E^2 - |\Delta(\mathbf{k})|^2}/E})} \quad (6)$$

We note that in the initial BCS formulation these u and v coefficients are only defined for $|E| > |\Delta(\mathbf{k})|$, but in this work we will extend this usage to energies $E < \Delta(\mathbf{k})$ including negative energy, and will model the effects of finite quasiparticle lifetime by letting $E \rightarrow E - i\Gamma$ ¹⁸, where Γ is the quasiparticle scattering rate. Note that this produces complex coherence factors whose squared amplitudes do not, in general, sum to unity. This is a consequence of the fact that

the transmitted waves in the superconductor are evanescent waves for $E < \Delta(\mathbf{k})$ and decay rapidly, with the electrons transmitted to the condensate⁹. These waves are effectively surface states. This extension of the coherence factors is crucial for studying the effects of tunneling voltages $V < \Delta(\mathbf{k})$, as are measured.

With the coherence factors in place, we are now in a position to consider the process whereby an incident electron in a normal metal undergoes Andreev and normal reflection at the N-S interface, with an electron-like quasiparticle and a back-scattered hole-like quasiparticle transmitted. This process is depicted in Figure 1. Note that the arrows indicate the particle group velocity; for the transmitted

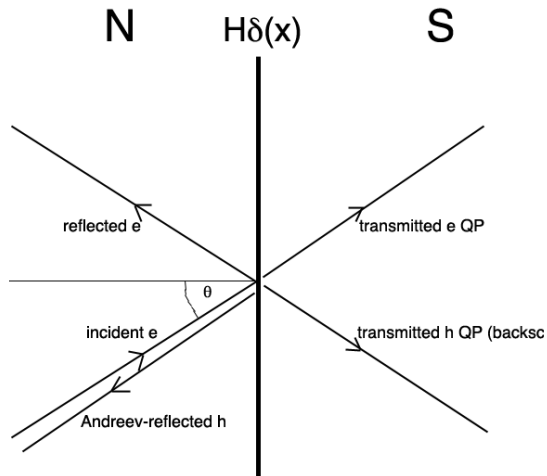


FIG. 1: A schematic diagram of all the particles involved in the reflection/transmission process at a N-S boundary; the arrows indicate the direction of the group velocity. Note that for the holes the momenta are opposite to this direction.

hole and Andreev-reflected hole the momentum is opposite to this. We have included a delta-function potential $H\delta(\mathbf{x})$ to model the inclusion of a thin oxide layer between the superconducting UPd_2Al_3 and the normal metal. Translational invariance parallel to the interface dictates that the momentum in this direction be conserved, while the momentum perpendicular to the interface is also conserved in the approximation where the barrier energy is much less than the Fermi energy of the incoming electron.

We note that unlike in virtually all other studies of the tunneling spectroscopy of unconventional superconductors, the Fermi momentum of the normal metal plays a key role in selecting the wavevectors which will contribute to the conductance, as indicated in Figure 2. Only a very small portion of the electrons in a spherical Fermi surface approximation will lie on the dominating, approximately cylindrical Fermi surface of UPd_2Al_3 , as indicated, and therefore contribute to the superconducting or normal state conductance. Electrons far from the Fermi surface cylinder of the UPd_2Al_3 will play no role.

We will also see that the conductance results depend critically on whether the wavevector selected lies near a nodal line; thus different

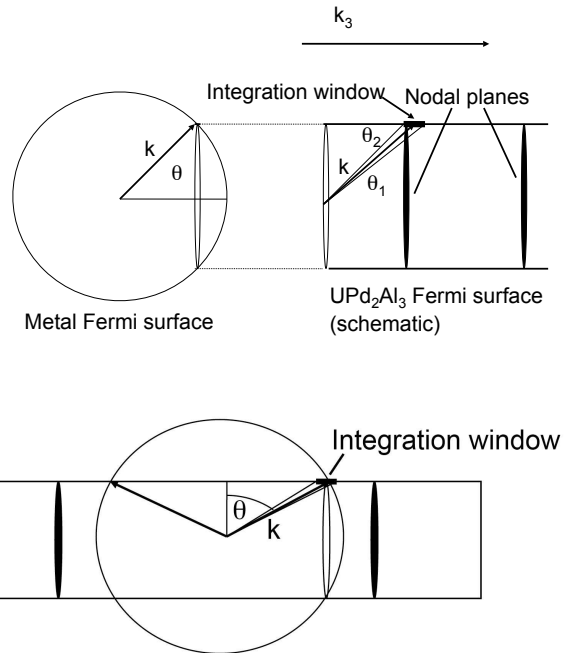


FIG. 2: A schematic diagram of the metallic and UPd_2Al_3 Fermi surfaces, for the longitudinal and transverse geometries. For the UPd_2Al_3 Fermi surface we take the main cylindrical sheet²⁰ and neglect its corrugation.

metals used on the normal side can be expected to display radically different behavior. Indeed, we will see that the measured gap magnitude, the zero-energy density-of-states, and even the existence of the usual coherence peaks will depend strongly upon the metal used. Finally, we have corrected for the effects of the electron effective mass mismatch¹⁹ at the interface.

III. CALCULATION METHODOLOGY

In our calculations we follow the work of Blonder et al⁹, Honerkamp and Sigrist¹⁴, and Tanaka¹¹. The basic method is straightforward: apply the usual boundary conditions at the interface and solve for the amplitudes of the various components.

The incoming electron wavefunction can be written as $\binom{0}{1} e^{ik_F x \cos \theta}$, with θ the angle between the normal to the interface and \mathbf{k} . We have suppressed the part of the wavefunction depending on the momentum parallel to the interface, as due to the translational invariance in this direction all of the involved momenta are equal. On the normal metal side, the Andreev-reflected hole, with amplitude a , has wavefunction $\binom{0}{1} e^{ik_F x \cos \theta}$, and the normally-reflected electron, with amplitude b , has wavefunction $\binom{1}{0} e^{-ik_F x \cos \theta}$. On the superconducting side, the electron-like quasiparticle, with amplitude c , has wavefunction $\binom{u(\theta)}{\exp(-i\phi_\theta)v(\theta)} e^{ik_F x \cos \theta}$, and the backscattered hole-like quasiparticle has wavefunction $\binom{\exp(i\phi_{\pi-\theta})v(\pi-\theta)}{u(\pi-\theta)} e^{ik_F x \cos \theta}$. Here the exponential factors represent the phase of the gap at the indicated angle. We are now able to apply the boundary conditions. Continuity of the wavefunction at the interface yields the first two of four equations

for the four unknowns a,b,c and d.

The usual boundary condition^{9,11} appropriate for a delta-function potential $H\delta(x)$ is

$$\psi'_S(0) - \psi'_N(0) = \frac{2m}{\hbar^2} H\psi(0) \quad (7)$$

However, due to the large effective mass mismatch at the boundary ($m_S \sim 100m_0$) we must generalize this condition. Integrating the Bogolubov-deGennes equations across the boundary we find

$$\frac{\psi'_S(0)}{m_S} - \frac{\psi'_N(0)}{m_N} = \frac{2}{\hbar^2} H\psi(0) \quad (8)$$

with the effective masses as indicated. Substituting the wavefunctions outlined above into this formula leads to the final two equations for the four unknowns a, b, c, and d. We find the following solutions for a and b:

$$a(\theta, E) = \frac{uv}{D} \quad (9)$$

with

$$D = (u^2 - e^{i(\phi_{\pi-\theta} - \phi_\theta)} v^2) |Z|^2 m + u^2 \quad (10)$$

$$b(\theta, E) = \frac{(u^2 - e^{i(\phi_{\pi-\theta} - \phi_\theta)} v^2) (|Z|^2 + Z)}{D} \quad (11)$$

Here $m = m_S/m_N$ and $Z = H/(iv_F \cos \theta) + 1/2m - 1/2$ where v_F is the metallic Fermi velocity, and $e^{i\phi} = \frac{\Delta(\theta)}{|\Delta(\theta)|}$, i.e. the gap phase. The energy dependence of a and b is contained in the coherence factors u and v. We note two interesting effects:

- The denominator D increases rapidly with mass mismatch m and effective barrier height Z. There are therefore narrow transmission resonances when the prefactor of the $|Z|^2 m$ term vanishes. For all the order parameters under consideration, the factors u_θ and $u_{\pi-\theta}$ are identical, as are v_θ and $v_{\pi-\theta}$. When the phase factor is unity, i.e. there is no change of order parameter sign under the change in angle from θ to $\pi - \theta$, the prefactor can only vanish when $u=v$, i.e. $E = \Delta(\mathbf{k})$. Thus for the two cosine-containing order parameters, we expect coherence peaks in the differential conductance at the gap energy selected by the wavevector matching on the UPd₂Al₃ Fermi surface. This implies that the energy, or voltage, of the conductance coherence peaks for these order parameters is a function of the normal metal's Fermi wavevector, in contrast to most tunneling spectroscopy studies, where no effects of wavevector matching are considered, because the Fermi surface on the superconducting side is also considered spherical. It is the peculiar geometry engendered by the longitudinal Fermi surface of UPd₂Al₃ that creates this unusual coherence peak effect.
- For the two sine-containing order parameters, the phase factor is -1, so that for a resonance we must satisfy $u^2 = -v^2$. Strictly speaking this is impossible, since $u^2 + v^2 = 1$, but the factors u and v diverge as $|E| \rightarrow 0$, so that both the numerator of $a(E, \theta)$ and the second term of D diverge, while the first term of D remains finite. As $E \rightarrow 0$, explicit calculation shows that, for $\Gamma = 0$ we attain perfect transmission, and therefore, we expect zero-energy resonances to appear as zero-bias conductance peaks for these two order parameters.

Following BTK and Tanaka^{9,11}, the normalized conductance at temperature $T = 1/\beta$ is given by

$$dI/dV = \sigma(V) \equiv \frac{\sigma_S(V)}{\sigma_N(V)} \quad (12)$$

$$= \frac{\int_{-\infty}^{\infty} dE \int_{\theta_1}^{\theta_2} d\theta \text{sech}^2(\beta(E-V)/2) (1 + |a(\theta, E)|^2 - |b(\theta, E)|^2)}{\int_{-\infty}^{\infty} dE \int_{\theta_1}^{\theta_2} d\theta \text{sech}^2(\beta(E-V)/2) \sigma_N(E)} \quad (13)$$

Note that we are not integrating over the full range of angles θ as the majority of such angles will result in wavevectors lying away from the nearly cylindrical²⁰ Fermi surface of UPd₂Al₃. In practice what we have done in all cases is to use the metallic Fermi momentum to determine the angle at which this momentum lies on the UPd₂Al₃ Fermi surface and then computed k_{z0} (the component of this momentum along the Fermi surface). As a rough accounting for actual metallic Fermi surface deviations from spherical we have then integrated over angles corresponding to k_z from 0.95 to 1.05 k_{z0} . For alkali metals such as sodium,³⁰ this is an overestimation, while for other materials - such as tungsten - this understates the Fermi surface deviations from spherical. Nevertheless, the results of our calculations are not sensitive to the size of the integration window used, provided that this window is small compared with the distance between the nodal planes. For all calculations we have taken the effective mass mismatch m as 100, while the barrier height H/v_F has been taken as unity. The results are not sensitive to either of these parameters.

IV. ORDER PARAMETER PROPOSALS

Before presenting the results of our calculations we give a brief summary of the order parameters which have been proposed for UPd₂Al₃. Note that in all proposals k_3 is taken as perpendicular to the ab-plane, and c is the c-axis lattice constant.

Won et al²³ proposed $\Delta(\mathbf{k}) = \cos(2ck_3)$ based upon magnetothermal conductivity data⁸, while McHale et al²¹ performed a strong-coupling calculation and found that both $\cos ck_3$ and $\sin ck_3$ had the highest transition temperatures, among possible order parameters. It was noted²² that the chiral order parameter $\exp(i\phi) \sin ck_3$ where $\exp(i\phi) = \hat{k}_1 + i\hat{k}_2$, is also a possible candidate. All of these order parameters contain nodal lines perpendicular to the k_3 axis, which were found in magnetothermal conductivity⁸ measurements on this material.

We note that the last two order parameters are odd under reflection around the basal plane; for all order parameters this reflection is equivalent to replacing θ in Figs. 1 and 2 and the above equations by $\pi - \theta$ (note that this is equivalent to reflection around $\theta = \pi/2$). This is immediately apparent for $\sin ck_3$, and the geometric diagram below shows that it is true for $\exp(i\phi) \sin ck_3$. Hence, when the tunneling is along the k_3 axis, this sign change is expected to produce zero-bias conductance peaks (ZBCP)¹¹ in the tunneling conductance. We will see that this is indeed the case.

V. RESULTS

Below in Fig. 4 is presented the normalized differential conductance dI/dV for the four order parameters described above, for the case where the tunneling direction is along the c-axis and the normal metal is lead, and $T \ll T_c$. These are the conditions of the experimental data at $T = 0.3\text{K}$ by Jourdan et al¹. We have here taken the quasi-particle lifetime broadening factor Γ to be $54 \mu\text{V}$, which compares well with that extracted from de Haas-van Alphen measurements²⁰, which measured Dingle temperatures of 0.1 - 0.28 K, corresponding to $\Gamma = 27 - 76 \mu\text{V}$. We find excellent agreement with the data of Jourdan et al¹ throughout the whole range modeled for the order parameters $\cos(ck_3)$ and $\cos(2ck_3)$, while contrary to experiment, a ZBCP is

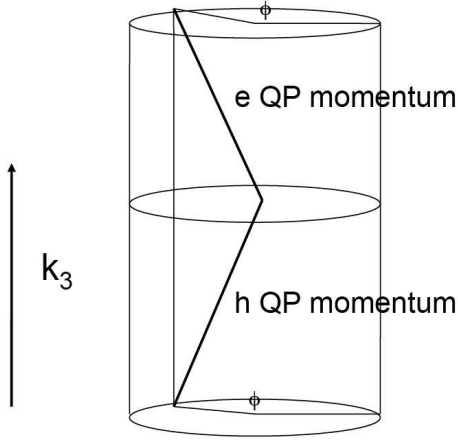


FIG. 3: A schematic diagram of the wavevector geometry for the chiral order parameter $\Delta(\mathbf{k}) = e^{i\phi} \sin(ck_3)$. Here k_3 is along the vertical axis. Note that the transmitted hole-like and electron-like quasiparticles have the same value of the phase ϕ , so that no additional phase is introduced by the chiral factor and the results are identical to the $\sin(ck_3)$ case.

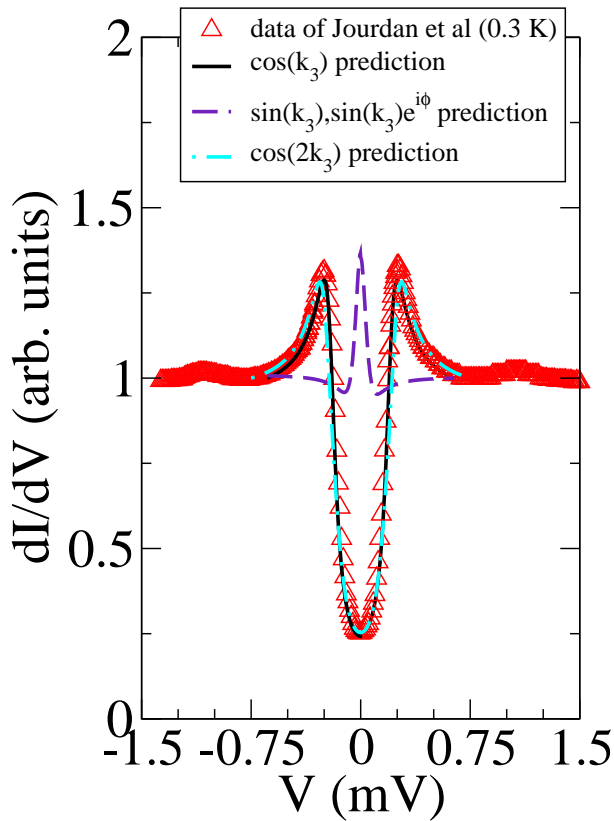


FIG. 4: The tunneling data of Jourdan at 0.3 K, with lead as the normal metal, is compared with predictions for the four order parameters shown.

predicted for the two sine-containing order parameters. Based on this data we thus believe it is rather unlikely that either of these two order

parameters is relevant for UPd_2Al_3 , although based upon calculations by Nishikawa²⁴ the $\sin(ck_3)$ gap function may have relevance for the isostructural superconductor UNi_2Al_3 . This material has indeed been proposed as a triplet superconductor having an odd gap function.²⁵

For completeness, we have computed dI/dV in the transverse direction, where the tunneling current is in the basal plane, with the same parameters as above. The results are shown in Fig. 5. As in the first plot, there is little difference between the two cosine order parameters, while the $\sin(ck_3)$ result shows virtually no coherence peak and no ZBCP, but a high zero-energy density-of-states (ZDOS). This is a direct result of the selected angle of incidence for lead in this geometry falling very near the nodal line for this order parameter; this property will be used to full advantage in proposing an experiment to distinguish between the two cosine order parameters. We have also performed calculations for the $\cos(ck_3)$ gap function

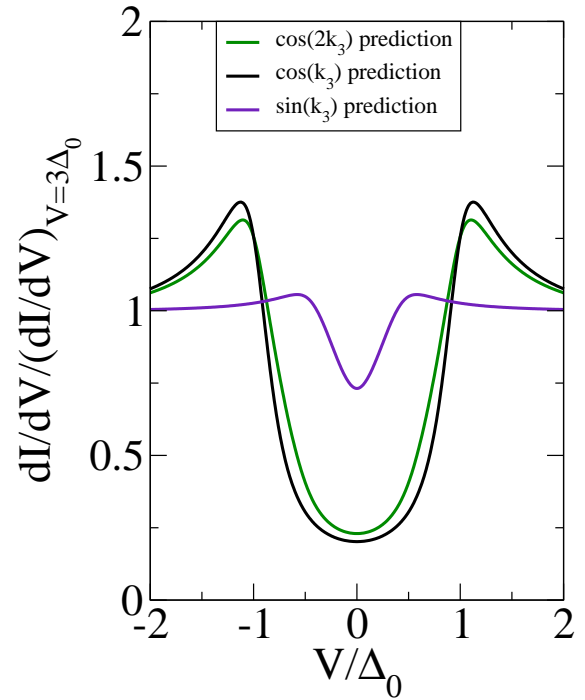


FIG. 5: The predictions for the ab-plane tunnelling conductance for the three order parameters indicated are shown.

for the entire range of temperatures tested by Jourdan et al, from 0.3 K to 1.5 K (in this experiment, T_c was 1.6 K.). Figure 6 below shows excellent agreement with this order parameter over the entire temperature range, for nearly all energies. We stress that this was accomplished with a minimum of fitting parameters; the quasiparticle lifetime broadening rate Γ was assumed temperature-independent ($\approx 54\mu\text{V}$) and the maximum energy gap value $\Delta(T)$ for all temperatures was near the value appropriate for BCS weak-coupling superconductors of this pairing symmetry^{26,27}. Below we have plotted the fitted values of $\Delta(T)$ compared to the BCS prediction. We note that based upon the fits of these data, the ratio $2\Delta(0)/T_c$ is approximately 3.7, indicating that a weak-coupling treatment may be accurate for this calculation. For this order parameter, in the weak-coupling limit the ratio $2\Delta(0)/T_c$ is 4.3. We also note, however, the slight bump in the data of Jourdan in Fig. 4 around $V = 1\text{mV}$, which may be indicative of strong-coupling to a magnetic-exciton boson^{21,28}.

We have not performed detailed comparison with experiment for

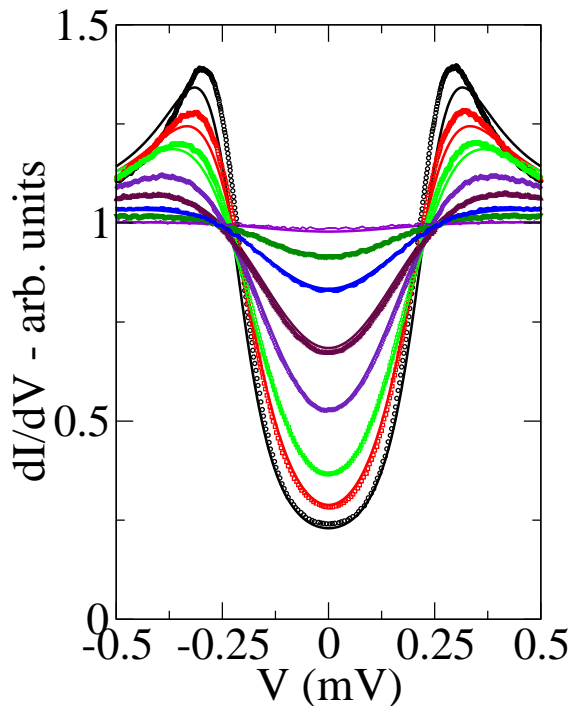


FIG. 6: The fits to the data of Jourdan using the $\cos(ck_3)$ order parameter are shown.

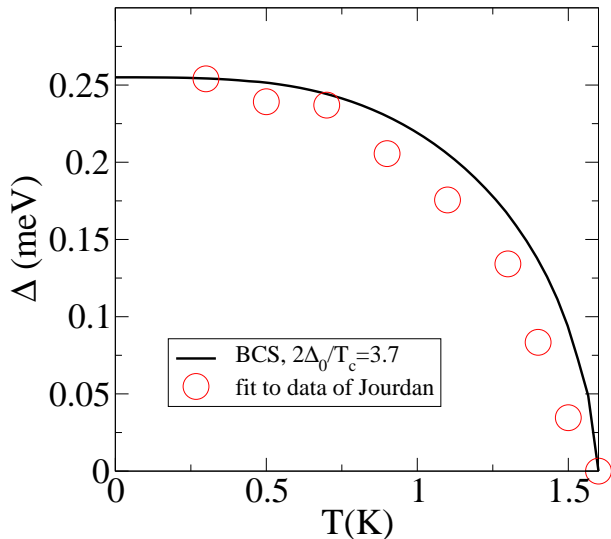


FIG. 7: The fitted values of $\Delta(T)$ are shown.

the $\cos(2ck_3)$ order parameter, although it is quite possible that similar agreement with experiment could be obtained for this case. We believe that this order parameter may be less likely to apply for UPd_2Al_3 for the reasons presented in²⁸; namely, the formation of a resonance peak in inelastic neutron scattering²⁹ requires, in the magnetic exciton scenario, a sign change over points on the Fermi surface separated by the antiferromagnetic wave-vector $\mathbf{q} = \frac{\pi}{c}\hat{k}_3$ and this does not apply for this order parameter. Nevertheless, we have devised what we believe is a definitive experiment to finally determine the order parameter in UPd_2Al_3 after fifteen years² of study.

VI. PROPOSED EXPERIMENT - ORDER PARAMETER DETERMINATION

The proposed experiment makes use of the unusual Fermi surface geometry effects present for tunnelling in the c -axis direction. The matching of wavevectors in the metal and in UPd_2Al_3 places sharp constraints on which region of the UPd_2Al_3 Fermi surface is employed by the superconducting electrons. In particular, it is possible to choose the normal metal so that for the $\cos(2ck_3)$ order parameter, the selected wavevector lies very near the nodal line, while for the $\cos(ck_3)$ order parameter, the selected wavevector is much more distant from the nearest node. We have chosen Calcium for this purpose as its Fermi wavevector, based on a spherical Fermi surface approximation³⁰ lies very near a nodal line of $\cos(2ck_3)$ but is far from a nodal line of $\cos(ck_3)$. The same situation would apply for Thallium and Cesium, but these are soft and reactive metals³¹ that are not likely to be useful in forming a tunnel junction.

In Figure 8 we show the results of the calculation for calcium at $T=0$, with the same quasiparticle lifetime broadening factor as before. We observe that for the $\cos(ck_3)$ case, reasonably well-

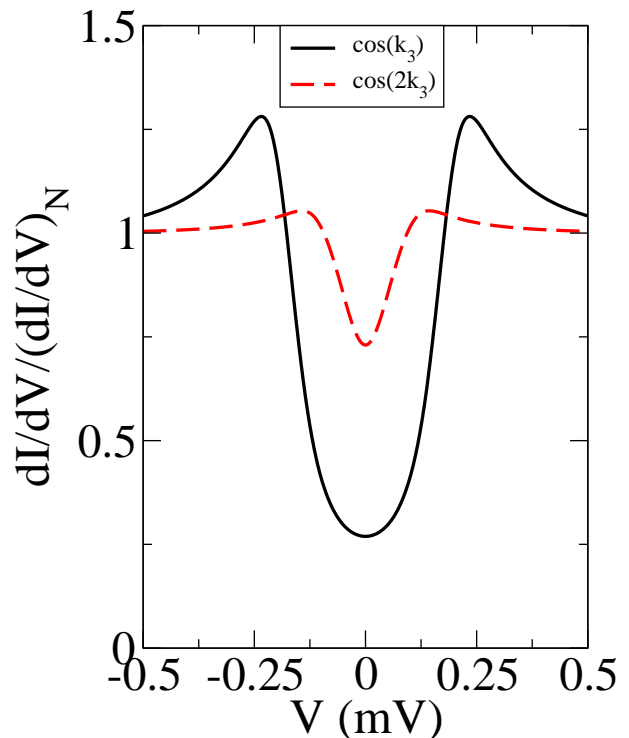


FIG. 8: Predictions for c -axis NS tunnelling with calcium as the normal metal are shown.

developed coherence peaks, at a magnitude of approximately $250\mu V$, and a comparatively low ZDOS (≈ 0.25) are present. However, for the $\cos(2ck_3)$ case, the coherence peaks are much broader and occur at significantly lower bias voltages ($V \approx 150\mu V$). In addition, the ZDOS is much higher - approximately 0.75. These differences are sufficiently robust that we believe that a calcium-based tunnel junction experiment, if technically feasible, would be sufficient to distinguish between these two order parameters.

For a final experiment of interest, we have computed the $T=0$ conductance for the $\cos(k_3)$ case for three metals commonly used in tunneling experiments - beryllium, gold, and aluminum - and show the results in Figure 9. As in the previous plot, the coherence peak height

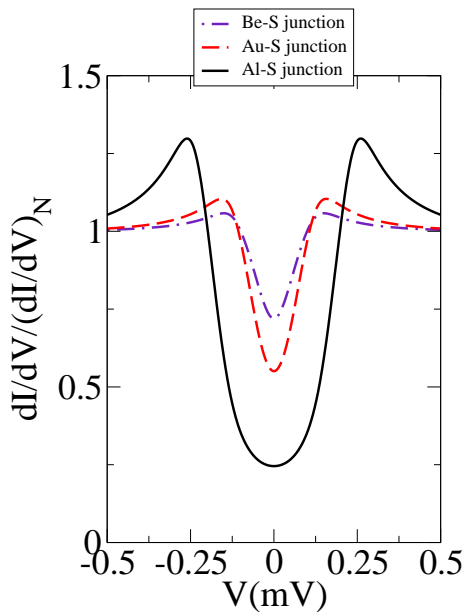


FIG. 9: Predictions for c-axis NS tunnelling for $\cos(ck_3)$ with beryllium, gold and aluminum as the normal metal are shown.

and energy vary greatly from one metal to another, with concomitant variations in the ZDOS. We believe that such experiments would be a good validation of the basic model employed in this paper, and would provide useful information regarding the assumption that only very few states on the UPd_2Al_3 Fermi surface contribute to the tunneling conductance.

VII. CONCLUSION

We have analyzed the tunnelling spectroscopy of the heavy-fermion superconductor UPd_2Al_3 , and studied four possible gap functions for this material: $\cos(ck_3)$, $\cos(2ck_3)$, $\sin(ck_3)$, and $\exp(i\phi)\sin(ck_3)$. We find that the last two gap functions would be expected to show zero-bias conductance peaks in c-axis tunnelling experiments as performed by Jourdan et al¹; these peaks were not observed and therefore these order parameters can be excluded. We further find that the $\cos(ck_3)$ order parameter gives an excellent fit to the experimental data of Jourdan at all temperatures, with a minimum of fitting parameters and a $\Delta(T)$ appropriate for the weak-coupling BCS theory of this material. Finally, we propose a definitive experiment to distinguish between the $\cos(ck_3)$ and $\cos(2ck_3)$ order parameters.

- ¹ M. Jourdan, M. Huth and H. Adrian, *Nature* **398**, 47 (1999).
- ² C. Geibel, C. Schank, S. Thies, H. Kitazawa, C.D. Bredl, A. Böhm, M. Rau, A. Grauel, R. Caspary, R. Helfrich, U. Ahlheim, G. Weber and F. Steglich, *Z. Physik B* **84**, 1 (1991).
- ³ R. Feyerherm, A. Amato, F.N. Gyax, A. Schenck, C. Geibel, F. Steglich, N. Sato and T. Komatsubara, *Phys. Rev. Lett.* **73**, 1849 (1994).
- ⁴ H. Tou, Y. Kitaoka, K. Asayama, C. Geibel, C. Schank and F. Steglich, *J. Phys. Soc. Jpn.* **64**, 725 (1995).
- ⁵ K. Matsuda, Y. Kohori and T. Kohara, *Phys. Rev. B* **55**, 15223 (1997).
- ⁶ N. Sato (unpublished).
- ⁷ M. Hiroi, M. Sera, N. Kobayashi, Y. Haga, E. Yamamoto and Y. Onuki, *J. Phys. Soc. Jpn.* **66**, 1595 (1997).
- ⁸ T. Watanabe, K. Izawa, Y. Kahasara, Y. Haga, Y. Onuki, P. Thalmeier, K. Maki and Y. Matsuda, *Phys. Rev. B* **70**, 184502 (2004).
- ⁹ G.E. Blonder, M. Tinkham and T.M. Klapwijk, *Phys. Rev. B* **25**, 4515 (1982).
- ¹⁰ A.F. Andreev, *Sov. Phys. - JETP*, **19**, 1228 (1964).
- ¹¹ Y. Tanaka and S. Kashiwaya, *Phys. Rev. Lett.* **74**, 3451 (1995).
- ¹² J.Y.T. Wei, N.-C. Yeh, D.F. Garrigus and M. Strasik, *Phys. Rev. Lett.* **81**, 2542 (1998).
- ¹³ M. Tinkham, *Introduction to Superconductivity*, Dover (Mineola, New York), 2nd ed., 2004.
- ¹⁴ C. Honerkamp and M. Sigrist, *J. Low Temp. Phys.* **111**, 895 (1998).
- ¹⁵ P.G. deGennes, *Superconductivity of Metals and Alloys*, Addison-Wesley (Reading), 1989.
- ¹⁶ T.M. Klapwijk, G.E. Blonder and M. Tinkham, *Physica* **109-110B**, 1657 (1982).
- ¹⁷ J.R. Schrieffer, *Theory of Superconductivity*, Perseus (Reading), 1999.
- ¹⁸ R.C. Dynes, V. Narayanamurti and J.P. Garno, *Phys. Rev. Lett.* **41**, 1509 (1978).
- ¹⁹ K. Sengupta, I. Žutić, H.J. Kwon, V.K. Yakovenko and S. Das Sarma, *Phys. Rev. B* **63**, 144531 (2001).
- ²⁰ Y. Inada, H. Aono, A. Ishiguro, J. Kimura, N. Sato, A. Sawada, T. Komatsubara, *Physica B* **119**, 119 (1994); Y. Inada, A. Ishiguro, J. Kimura, N. Sato, A. Sawada, T. Komatsubara and H. Yamagami, *Physica B* **206-207**, 33 (1995); Y. Inada, H. Yamagami, Y. Haga, K. Sakurai, Y. Tokiwa, T. Honma, E. Yamamoto, Y. Onuki and T. Yanagisawa, *J. Phys. Soc. Jpn.* **68**, 3643 (1999).
- ²¹ P. McHale, P. Fulde and P. Thalmeier, *Phys. Rev. B* **70**, 014513 (2004).
- ²² Y. Matsuda, K. Izawa and I. Vekhter, *J. Phys.: Cond. Matt.* **18**, R705 (2006).
- ²³ H. Won, D. Parker, K. Maki, T. Watanabe, K. Izawa and Y. Matsuda, *Phys. Rev. B* **70**, 140509 (2004).
- ²⁴ Y. Nishikawa and K. Yamada, *J. Phys. Soc. Jpn.* **71**, 2629 (2002).
- ²⁵ K. Ishida, D. Ozaki, T. Kamatsuka, H. Tou, M. Kyogaku, Y. Kitaoka, N. Tateiwa, N.K. Sato, N. Aso, C. Geibel and F. Steglich, *Phys. Rev. Lett.* **89**, 037002 (2002).
- ²⁶ We note that the temperature dependence of the gap in the weak-coupling approximation is the same as for d-wave superconductors, as the Fermi surface angular averages $\langle f^2 \rangle$ and $\langle f^2 \ln |f| \rangle$, where $\Delta(\mathbf{k}) = \Delta(T)f(\mathbf{k})$, are identical. See Ref.²⁷.
- ²⁷ H. Won and K. Maki, *Phys. Rev. B* **49**, 1397 (1994).
- ²⁸ J. Chang, I. Eremin, P. Thalmeier and P. Fulde, *cond-mat/0609550*.
- ²⁹ N.K. Sato, N. Aso, K. Miyake, R. Shiina, P. Thalmeier, G. Varelogiannis, C. Geibel, F. Steglich, P. Fulde and T. Komatsubara, *Nature* **410**, 340 (2001).
- ³⁰ N.W. Ashcroft and N.D. Mermin, *Solid State Physics*, Thomson Learning (Singapore), 1976.
- ³¹ *Handbook of Chemistry and Physics*, D.R. Lide, (ed.), CRC Press (Boca Raton), 77th Edit. (1996).